Friction and Wear of Si_3N_4 Ceramic/Stainless Steel Sliding Contacts in Dry and Lubricated Conditions

X.Z. Zhao, J.J. Liu, B.L. Zhu, H.Z. Miao, and Z.B. Luo

Austenitic stainless steel AISI 321 is one of the most difficult-to-cut materials. In order to investigate the wear behavior of Si_3N_4 ceramic when cutting the stainless steel, wear tests are carried out on a pin-on-disk tribometer, which could simulate a realistic cutting process. Test results show that the wear of Si_3N_4 ceramic is mainly caused by adhesion between the rubbing surfaces and that the wear increases with load and speed. When oil is used for lubrication, the friction coefficient of the sliding pairs and the wear rate of the ceramic are reduced. A scanning electron microscope (SEM), an electron probe microanalyzer (EPMA), and an energy dispersive x-ray analyzer (EDXA) are used to examine the worn surfaces. The wear mechanisms of Si_3N_4 ceramic sliding against the stainless steel are discussed in detail.

Keywords
adhesive wear, lubrication, silicon nitride, stainless steel

1. Introduction

SILICON NITRIDE (Si_3N_4) based ceramics, because of their excellent thermal and mechanical properties, have attracted much attention as structural materials. One of the most important uses of Si_3N_4-base ceramics is for cutting tools, which are applied in turning cast iron and nickel-based alloys at high speeds (Ref 1, 2). However, the Si_3N_4-based ceramics have been found to be unsuitable for machining steel. One of the factors influencing this difference in behavior is thought to be chemical dissolution of the ceramics in the chip at the high temperatures reached at the cutting edge (Ref 3). The wear rate of a silicon nitride cutting tool is two orders of magnitude higher when machining AISI 1045 steel than when machining gray cast iron (Ref 4). The high cratering wear of sialon ceramics when machining AISI 1045 steel is caused by the chemical dissolution of sialon grains and followed by pull out of sialon grains from the glassy intergranular phase (Ref 5).

Austenitic stainless steels, one of the most widely used class of materials, are very different from carbon steel in many properties. However, little knowledge is available about the wear behaviors of Si_3N_4-base ceramics used for cutting austenitic stainless steels. The objective of this study is to investigate the wear behavior of a Si_3N_4-based ceramic on a pin-on-disk tribometer under dry and lubricated conditions. Compared with real machining tests, pin-on-disk tests are simple and quick. Since their conditions of solicitation may be widely varied and well controlled, pin-on-disk tests seem to be appropriate for tool life simulation. Some work has been done in the wear mechanism analysis of ceramic tool materials and the comparison of wear data from pin-on-disk tests and cutting behavior of ceramics (Ref 6, 7). In the present test, the worn surfaces of the Si_3N_4 ceramic are examined and analyzed by using a scanning electron microscope (SEM), an electron probe microanalyzer (EPMA), an energy dispersive x-ray analyzer (EDXA), and an x-ray photoelectron spectroscopy (XPS).

X. Zhao, J. Liu, B. Zhu, H. Miao, and **Z. Luo,** Tribology Research Institute, Tsinghua University, Beijing 100084, People's Republic of China.

2. Experimental Procedure

2.1 *Test Machine and Specimens*

Wear tests are carried out on a pin-on-disk tribometer. The pin specimen is fixed; the disk specimen, driven by a motor, rotates at different speeds. The contact model of the specimens is shown in Fig. 1. Initial line contact is formed between the pin and the disk, which can simulate well the contact form of cutting tool and workpiece in a realistic cutting practice. The pin is made from hot-pressed Si_3N_4 ceramic (containing Si_3N_4+TiC+Al_2O_3, where Si_3N_4 is >80 wt%), having a size of 5 × 5 × 25 mm. The disk is machined from AISI 321 stainless steel, 56 mm in diameter and 6 mm in thickness. The frictional surface roughnesses of the pin and the disk are Ra = 0.32 μm and Ra = 0.21 μm, respectively. Some properties of the Si_3N_4 ceramic are listed in Table 1.

Table 1 Physical and mechanical properties of the Si_3N_4 ceramic

Properties	Value
Density, g/cm^3	3.5
Hardness, HV	1900
Bending strength, MPa	750
Elastic modulus, GPa	290
Fracture toughness, MPa · m$^{1/2}$	6.3
Grain size, μm	<1.3

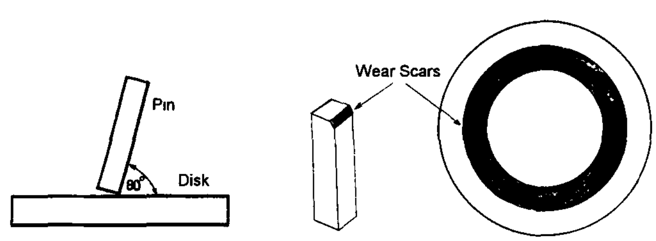

Fig. 1 Contact model and wear scars of the pin and disk

2.2 *Test Method*

Friction and wear tests are operated under dry and lubricated conditions, respectively. The room temperature is about 20 °C. A pure liquid paraffin is used for lubrication; its kinematic viscosity at 25 °C is 30 mm^2/s. During the operating process, the lubricating oils are fed into the contact point between the pin and the disk by natural falling flow from a reservoir. The average rate of the flow is about 0.01 L/min. The sliding speeds between the rubbing surfaces are 1.6 m/s and 3.2 m/s, and the selected load range is 58.8 N to 235.2 N. Each pair had a 30 min running time under the selected speed and load, and at least two tests are performed. Before and after testing, the specimens are ultrasonically cleaned in acetone bath for 15 min and then in hexane bath for 2 min.

The wear scar width of the pin is measured under a photomicroscope, so the volume and wear rate can be calculated. The friction force is transmitted by a transducer to a recorder continuously during the test, from which the friction coefficient can be obtained. The worn surfaces are examined by SEM, EDXA, and XPS.

3. Results and Discussion

3.1 *Effects of Load on Friction Coefficient and Wear Rate*

Figures 2 and 3 show the variation of friction coefficient and the wear rate with load, respectively. The friction coefficient and wear rate of the ceramic increase with load under both dry and lubricated conditions. However, when oil is used for lubrication, the friction coefficient decreases by ⅓, and the wear rate decreases about two orders of magnitude. In dry conditions, stainless steel transfers onto the worn ceramic surfaces at both low and high loads. The rapid increase of the wear rate under dry conditions at a higher load (235.2 N) might be caused by severe adhesion between the rubbing surfaces and the increase of the microfracture of the ceramic, which was confirmed by the SEM examinations of the worn Si_3N_4 ceramic surface and the wear debris (see Fig. 4a, 4b, and the microfracture fragments in Fig. 5). (The arrow in Fig. 4a points to the microfracture pit.) The EDXA spectrum of the fragment in Fig. 5 is shown in Fig. 6. The element compositions indicate that the

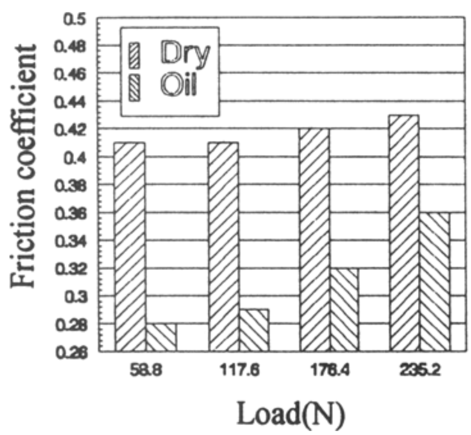

Fig. 2 Variation of friction coefficient with load

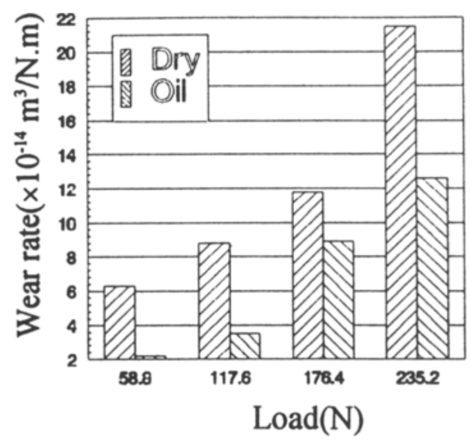

Fig. 3 Variation of wear rate of the ceramic with load

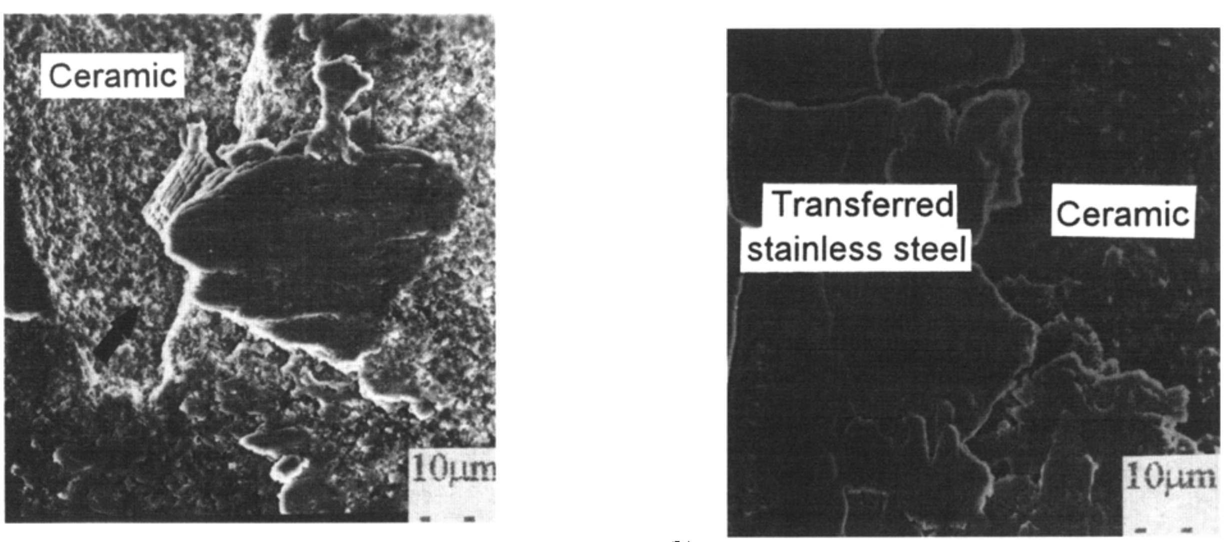

(a) **(b)**

Fig. 4 SEM morphologies of the worn ceramic surfaces (dry, 235.2 N, 1.6 m/s) particle came from Si_3N_4 ceramic. For comparison, the SEM morphology of the worn Si_3N_4 surface of lower load is shown in Fig. 7.

Under lubricated conditions, the amount of transferred stainless steel on the worn ceramic surfaces was much less than under dry conditions, and little microfracture occurred even at higher load (see Fig. 8). In addition, the worn stainless steel surface of lubricated conditions is smoother than that of dry conditions (see Fig. 9). The stainless steel wear debris in dry and lubricated conditions is also different in shape and size (see Fig. 10). In dry frictional conditions, the wear debris through creep becomes deformed, block-shaped, and bigger in size, especially at higher load. While in oil-lubricated conditions, most of the wear debris is long, belt-shaped, and smaller in size. The results show that the adhesion between the rubbing surfaces is reduced to great extent by the lubricating oil; the friction coefficient and cutting force are also reduced. Reference 8 shows that lubricating oils can increase the critical fracture load of ceramics, which is also confirmed by the results of this test. The wear rate of Si_3N_4 ceramic is reduced much more at higher load in comparison to dry friction conditions.

3.2 *Effects of Speed on Friction Coefficient and Wear Rate*

The variations of friction coefficient and wear rate with speed are shown in Fig. 11 and 12. Similar to the effects of load, under dry conditions the friction coefficient and wear rate increase with speed. However, the friction coefficient increases more rapidly and reaches a much higher value compared with the effect of load. High speed brings about a large amount of friction heat, which aggravates the adhesion between the rubbing surfaces, so both the friction coefficient and wear rate in-

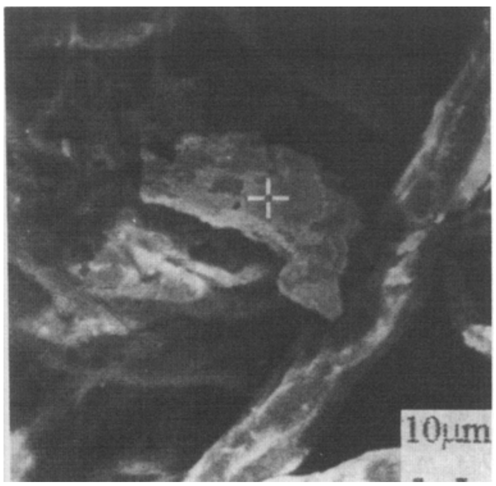

Fig. 5 SEM examination of microfracture fragments (dry, 235.2 N, 1.6 m/s)

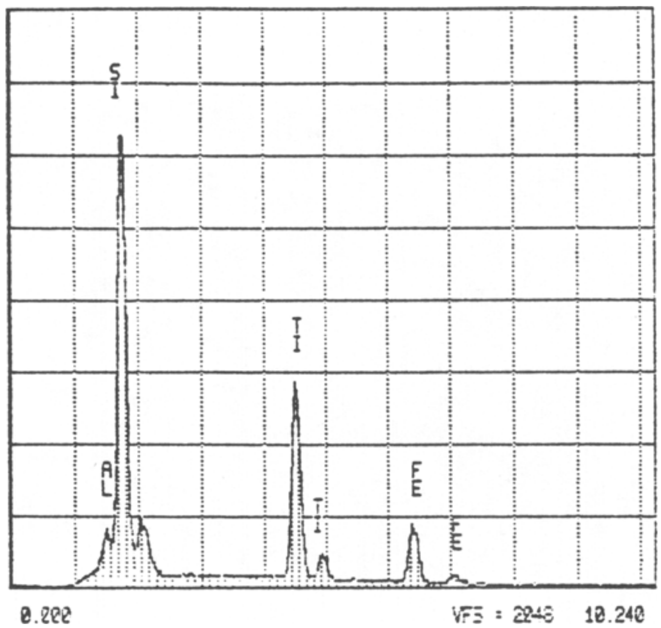

Fig. 6 EDXA spectrum of the fragment in Fig. 5

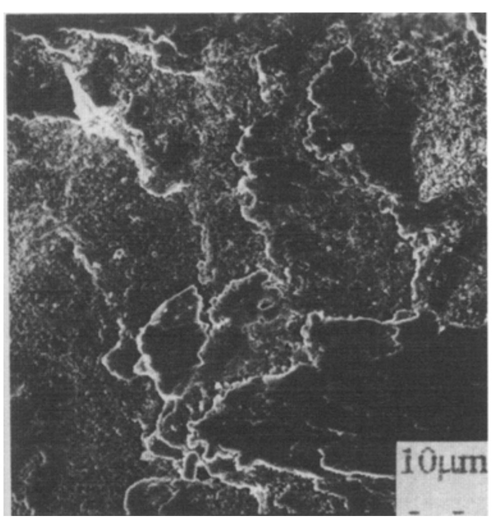

Fig. 7 SEM morphology of the worn ceramic surface (dry, 117.6 N, 1.6 m/s)

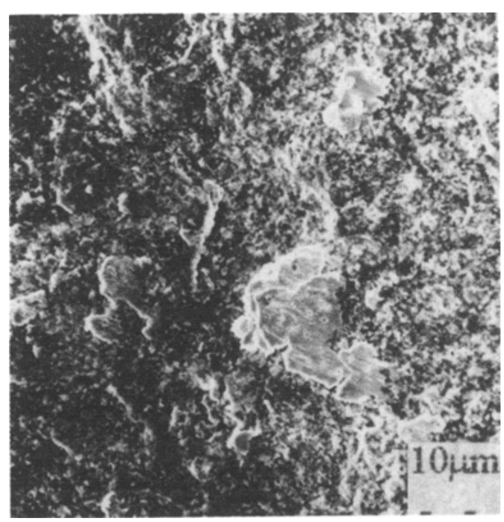

Fig. 8 SEM morphology of worn ceramic surface (oil-lubricated 235.2 N, 1.6 m/s)

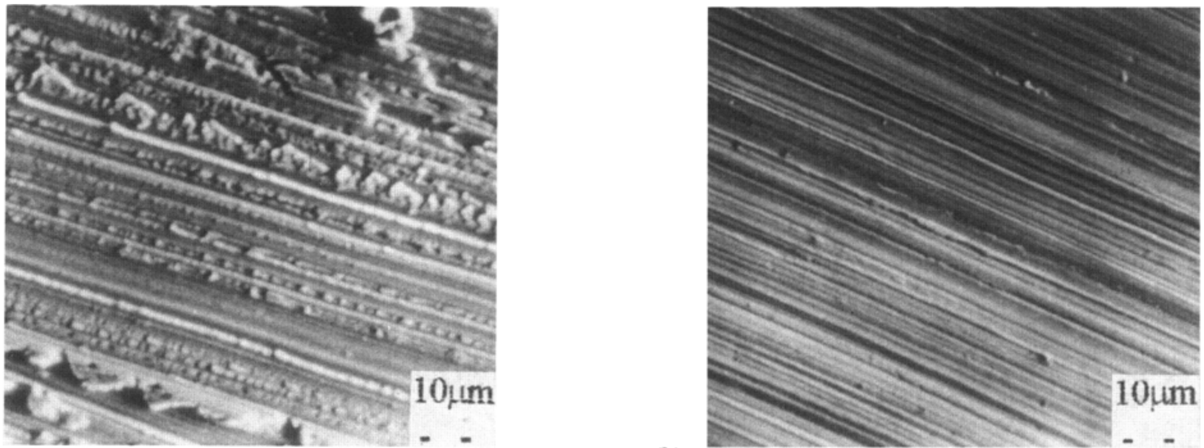

(a) (b)

Fig. 9 SEM morphologies of worn stainless steel surfaces. (a) Dry condition. (b) Oil-lubricated condition

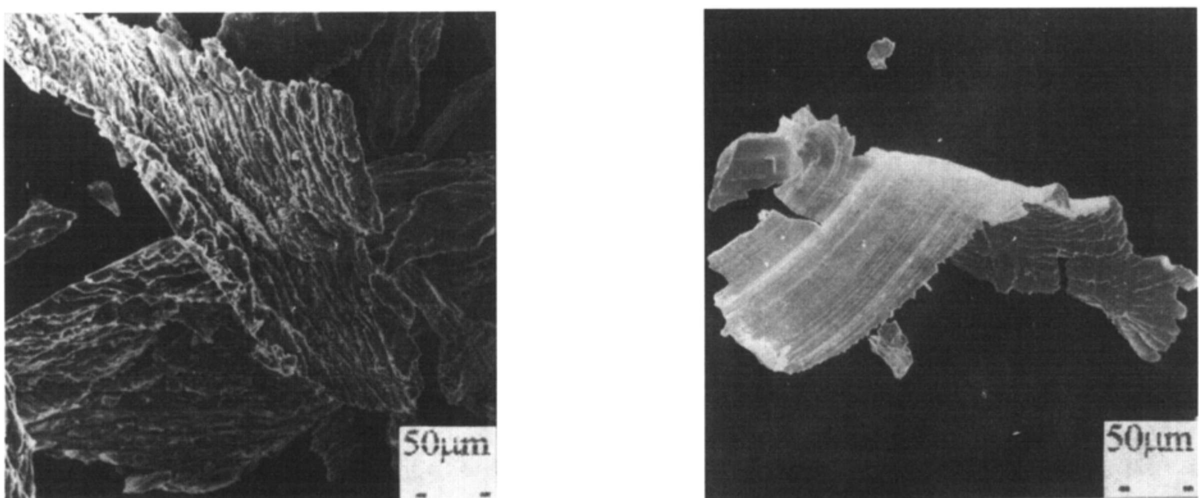

(a) (b)

Fig. 10 SEM morphologies of stainless steel wear debris. (a) Dry condition. (b) Oil-lubricated

crease with speed. In general, the SEM morphologies of the worn Si_3N_4 surfaces obtained at different speeds are similar to Fig. 4 and 7. (Stainless steel transfer on the worn ceramic surfaces also occurs at different speeds.) At high speed (3.2 m/s in this test), some ceramic grains melt on the worn ceramic surfaces (see section 3.4 for details). Compared with dry conditions, the friction coefficient and wear rate are reduced because of the lubricating and cooling effects of the lubricating oil. This result is consistent with the result of Ref 9, that lubricating oils are quite effective in reducing the friction coefficient and wear rate of ceramics in ceramic/metal sliding pairs.

3.3 *Wear Mechanisms of Si_3N_4 Ceramic Sliding on Austenitic Stainless Steel*

In order to reveal the wear mechanism of Si_3N_4 ceramic, SEM is used to examine the worn surfaces. The SEM morphologies of the worn ceramic surfaces at different loads are shown in Fig. 4 and 7. Stainless steel transfers onto the ceramic surfaces because of adhesion between the rubbing surfaces. Figures 4 and 7 also show that the amount of the transferred stainless steel increases with load and that many larger transferred stainless steel flats formed on the worn ceramic surface at a higher load (235.2 N). Only smaller stainless steel flats are formed at a lower load (117.6 N).

From the examinations, one can deduce the wear process of the ceramic. A high chemical affinity exists between iron and silicon nitride (Ref 10, 11), and strong adhesion will occur when Si_3N_4 and stainless steel are put into sliding contact. With the relative movement of the rubbing surfaces, the adhesion points or areas are torn off, resulting in the transfer of stainless steel onto the rubbing ceramic surface. (The adhesive points or areas are broken more frequently in a stainless steel surface because of its relatively low shearing strength.)

The transferred stainless steel on the ceramic surface is subjected to repeated shearing and compressive stresses by the rubbing movement, causing microcracks and microfractures in the ceramic surface or its subsurface. Meanwhile, the transferred stainless steel is also subjected to adhesive force coming from the rubbing stainless steel surface, which peels off the

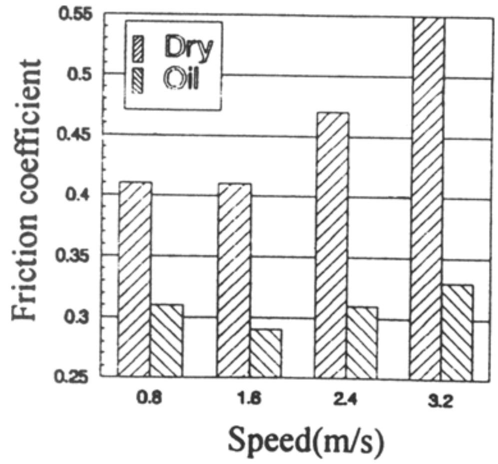

Fig. 11 Variation of friction coefficient with speed

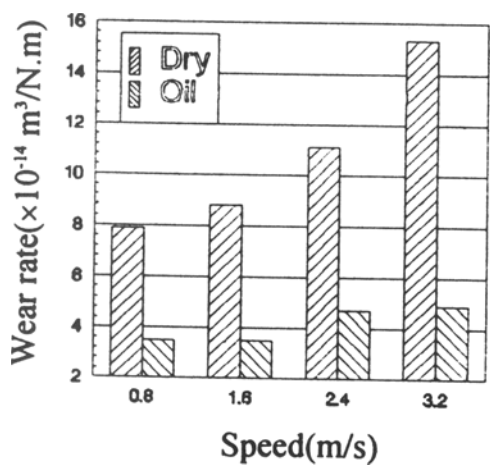

Fig. 12 Variation of wear rate of the ceramic with speed

transferred stainless steel flats. Ceramic microfracture pieces or Si_3N_4 grains are also peeled off or pulled out and leave the ceramic surface with the peeled off stainless steel flats, giving rise to the wear of the ceramic.

The adhesion peeling-off mechanism of the ceramic wear can be confirmed by the EDXA analysis result of the wear debris (see Fig. 13a, b). The intense Si peak in Fig. 13(b) shows the wear debris is not only stainless steel but rather is a combination of Si_3N_4 particles and stainless steel brought together by adhesion.

3.4 *Chemical Wear of Si_3N_4 and Melting of Some Ceramic Grains*

In addition to the adhesion peeling-off mechanism, the wear of the ceramic is also attributed to chemical wear, oxidation of the Si_3N_4 grains. The XPS analysis showed that SiO_2 (the oxidation product of Si_3N_4 in rubbing process) is produced on the worn ceramic surface. (The binding energy of Si 2p is 103.3 eV.) EPMA examinations find some microballs on the worn Si_3N_4 surfaces (see Fig. 14a). Composition distribution analyses corresponding to Fig. 14(a) are shown in Fig. 14(b) to (d).

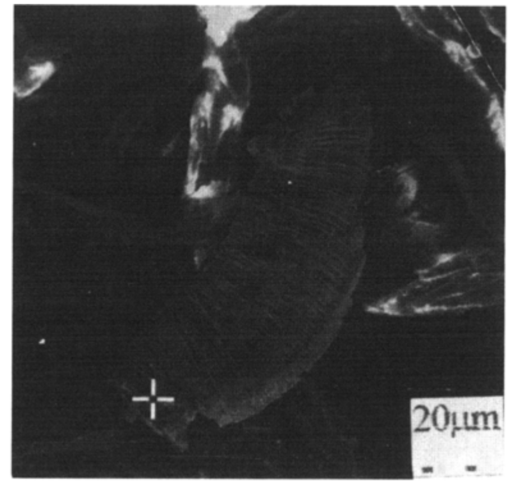

(a)

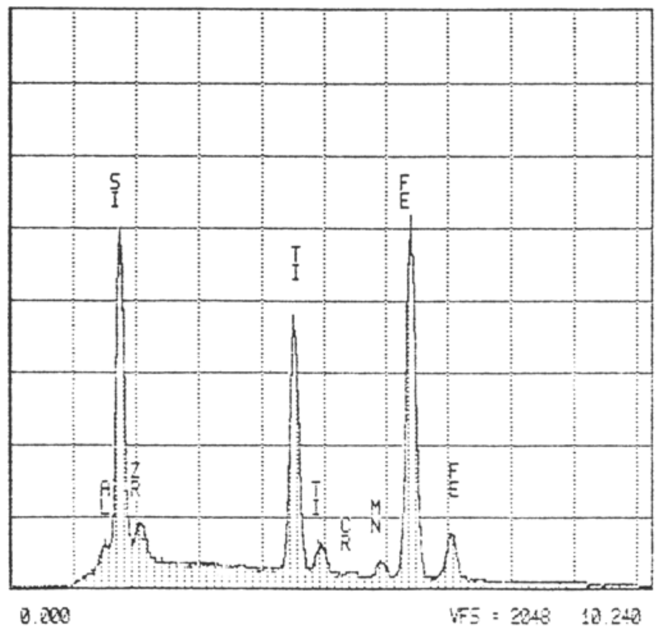

(b)

Fig. 13 (a) SEM morphology of the wear debris. (b) EDXA spectrum of the marked point in (a)

These analyses suggest that the microballs might come from molten SiO_2 (Si_3N_4 is more easily oxidized than melted), TiC grains, and stainless steel, respectively. Although Si_3N_4, SiO_2, and TiC have high melting points, the ceramic grains can still melt due to the following factors. The worn ceramic surface is not only composed of Si_3N_4, SiO_2, and TiC, it also contains a lot of additives, such as CaO and Y_2O_3, that reduce the melting point of the ceramic. In other words, some low melting point eutectics are formed in the rubbing process. This melting phenomena is consistent with the results of Ref 12. According to the Fe-Si diagram, a liquid phase exists at 1200 °C, and two eutectics are present at 1085 and 1289 °C, respectively, in the Fe-Ti phase diagram (Ref 13). These temperatures might have been reached at higher sliding speed in this test. The heat conductivity of the ceramic is rather bad, and a large amount of de-

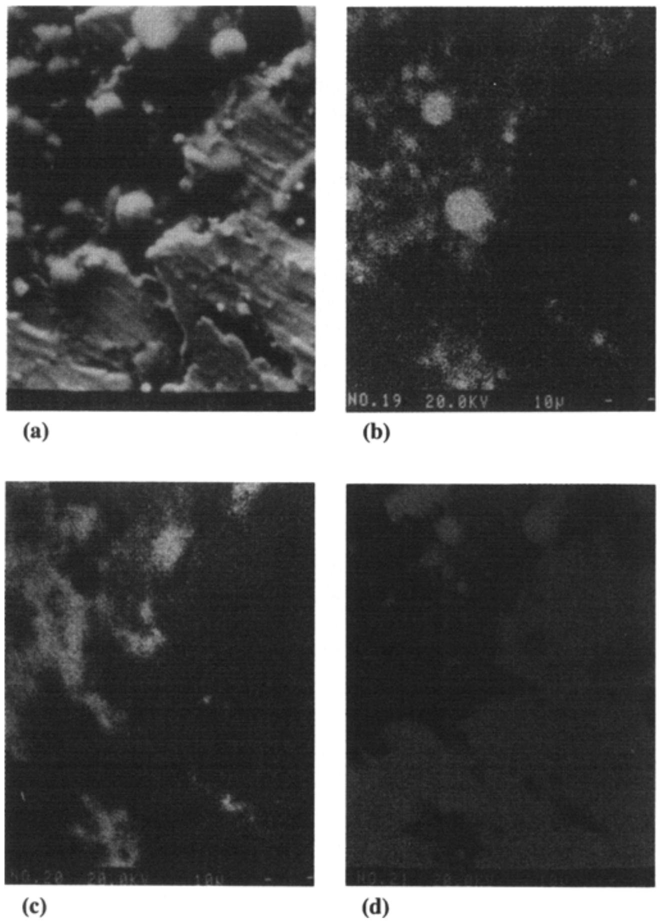

Fig. 14 EPMA examinations of the worn ceramic surfaces (dry, 117.6 N, 3.2 m/s). (a) Microballs. (b) Si distribution. (c) Ti distribution. (d) Fe distribution

formation and friction heat is produced in rubbing process. In addition, since the small contact area of the ceramic sample maintains contact during the entire rubbing process, the temperature of its contact surface might be much higher than that of the stainless steel surface. According to Ref 7, the chemical dissolution of Si_3N_4 grains in wear chip is more severe, because the stainless steel has higher toughness and lower heat conductivity than AISI 1045 steel, which also accelerates the melting of the ceramic grains.

Adhesion, melting, and element diffusion are not isolated; they are relative to each other. With increasing load and speed, real contact area and friction heat increase, in turn accelerating the melting of the ceramic grains and the element diffusion, and thus resulting in heavy adhesive wear. When an oil is used for lubrication, the lubricating and cooling actions of the oil decrease the adhesion between the rubbing surfaces, the temperature of the rubbing surfaces, and the element diffusion, so the friction coefficient and wear rate are reduced.

4. Conclusions

From the above test results and surface examinations, the following conclusions can be made:

- In Si_3N_4 ceramic/stainless steel sliding contacts, the wear of the ceramic is mainly caused by the adhesion peeling-off process. Stainless steel first transfers onto the ceramic surface. Then the transferred stainless steel flats are subjected to repeated shear and compressive stresses until they are peeled off the rubbing ceramic surface. When the transferred stainless steel flats are peeled off the ceramic surface, some ceramic fragments or grains are also pulled out and taken away. The higher load brings about more severe adhesive and microfracture wear of the ceramic.
- The melting of the ceramic grains and the element diffusion also cause the wear of the ceramic. However, they also aggravate the adhesion between the rubbing surfaces and thus result in more severe adhesive wear of the ceramic.
- With increasing load and speed, the friction heat of the rubbing surfaces increases rapidly, in turn accelerating the melting of the ceramic grains, element diffusion, and adhesion between the rubbing surfaces, so the wear of the ceramic increases with load and speed.
- Because of its lubricating and cooling actions, the oil reduces the friction coefficient and wear rate of the Si_3N_4 ceramic/stainless steel sliding pairs. This result suggests that appropriate lubrication and cooling are useful and helpful for the wear reduction of Si_3N_4-based ceramic cutting tools in real cutting processes, on which more research certainly should be done in the future.

Acknowledgments

The authors would like to thank the National Natural Sciences Foundation of China and the Laboratory of Solid Lubrication, Lanzhou Institute of Chemical Physics, Chinese Academy of Sciences, for their financial support to this project.

References

1. T.N. Blackman, *Foundryman,* Vol 3, 1990, p 17-24
2. J. Aucote and S.R. Foster, *Mater. Sci. Technol.,* Vol 2, 1986, p 700-708
3. J. Vleugels et al., *Mater. Sci. Eng.,* Vol A187, 1994, p 177-182
4. E.K. Asibu, *J. Manuf. Systems,* Vol 9, 1990, p 159-168
5. M.K. Brun and M. Lee, *Ceram. Eng. Sci. Proc.,* Vol 4, 1983, p 646-662
6. R. Rigaut, Y.M. Chen, and J. Saint Chely, *Lubr. Eng.,* Vol 50, 1994, p 485-489
7. G. Brant, A. Gerendas, and M. Mikus, *J. Eur. Ceram. Soc.,* Vol 6, 1990, p 273-290
8. D.H. Buckley and K. Miyoshi, *Wear,* Vol 100, 1984, p 333-353
9. H.K. Tonshoff, H.G. Wobker, and D. Brandt, *Lubr. Eng.,* Vol 50, 1995, p 163-168
10. B.M. Kramer and N.P. Suh, *J. Eng. Ind.,* Vol 102, 1980, p 303-309
11. B.M. Kramer and P.K. Judd, *J. Vac. Sci. Technol.,* Vol A3, 1985, p 2439-2444
12. S.Lo. Casto, E.Lo. Valvo, V.F. Ruisi, E. Lucchini, and S. Maschio, *Wear,* Vol 160, 1993, p 227-235
13. T. Massalski, J.J.H. Bennet, and H. Baker, Ed., *Binary Alloy Phase Diagrams,* Vol 2, ASM International, 1987